

## Enhancing Hydro Turbine Frequency Regulation with Neural Network-Aided PID Governor Design

Nguyen Hong Quang <sup>\*</sup>, Nguyen Tuan Ninh

School of Electrical and Electronic Engineering, Hanoi University of Science and Technology, Ha Noi, Vietnam

<sup>\*</sup>Corresponding author email: quang.nguyenhong1@hust.edu.vn

### Abstract

This paper presents a novel approach to hydro turbine speed control by integrating neural networks into the tuning process of digital governors, with the objective of meeting the stringent performance requirements set by the National Power System Control Center of Vietnam Electricity (EVN). The proposed control strategy employs a closed-loop configuration using turbine rotational speed as feedback to regulate water flow and maintain power balance under varying load conditions. A key innovation of the study is the use of an adaptive neural network - proportional integral derivative (NN-PID) Controller, which continuously updates control parameters in real-time through the Brandt-Lin learning algorithm. This allows the controller to respond effectively to nonlinearities and disturbances in the system. Simulation and hardware-in-the-loop experiments validate the effectiveness of the proposed method, demonstrating enhanced performance compared to traditional proportional integral derivative (PID) controllers including faster settling times, zero steady-state error, and suppression of oscillations during sudden load changes. The results suggest that the NN-PID controller offers a promising alternative for next-generation digital governor design in large hydropower plants.

Keywords: PID, neural network, turbine governor

### 1. Introduction

Primary Frequency Control in Vietnam refers to the automatic and immediate response of power plants to stabilize the power system's frequency, typically maintained at  $50 \pm 0.5$  Hz, as mandated by Circular 40/2014/TT-BCT (amended by Circular 31/2019/TT-BCT) issued by the Ministry of Industry and Trade. It is a critical mechanism to balance electricity supply and demand in real-time when frequency deviations occur due to sudden changes in load or generation.

In practice, the generating unit of a power plant must be capable of participating in primary frequency control when the system frequency deviates beyond the deadband of the governor system. It must achieve at least 50% of the primary frequency control capacity of the unit within the first 15 seconds, 100% of the primary frequency control capacity within 30 seconds, and maintain this capacity for at least an additional 15 seconds.

The basic controller using in most of hydropower plants is the proportional integral derivative (PID) controller, in which the tuning method is using Ziegler-Nichol's algorithms as presented in [1]. However, the method for finding gains via an optimal control approach in [2] is time-consuming. The stability is not ensured for different loads.

This study introduces two alternative methodologies for optimizing turbine governor

parameter design. The first is a model-based controller design approach, effective when accurate and comprehensive data on the turbine-governor system are available. The process begins with developing a mathematical model of the system using differential equations. Controllers are then designed based on established PID control principles, with closed-loop poles selected to meet specific performance criterias such as overshoot, rise time, and settling time. This method yields analytical expressions for controller parameters as functions of system operating conditions and desired closed-loop behavior, thereby eliminating the need for heuristic tuning.

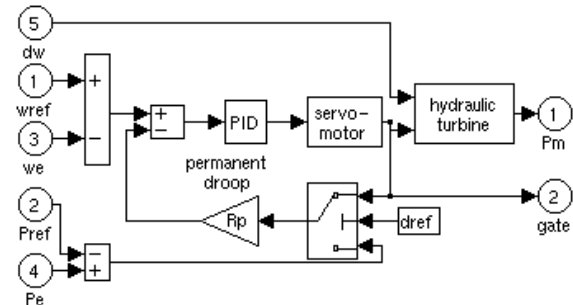
Simulation results indicate that the system experiences fluctuations in response to significant variations in input parameters, such as the water gross head, inaccurate estimation of the water time constant, or abrupt load changes. To address these phenomena, a novel approach involving the online calculation of PID controller parameters is proposed to satisfy the system's quality requirements [3]. The primary advantages of the proposed neural network-based method include its capacity for parallel processing and its ability to learn and approximate arbitrary nonlinear functions. This paper provides a comprehensive derivation of the neural network-based PID controller specifically designed for turbine power control applications.

The validation of the proposed controllers is conducted using a hardware-in-the-loop model implemented within MATLAB Real-Time Workshop. This design facilitates the simulation of a broad and significant range of operating conditions, including turbine startup, normal and emergency shutdown, no-load generation, and parallel operation under short-circuit scenarios. Furthermore, the integration of the excitation system with supplementary control loops such as Power System Stabilizer (PSS), under excitation, and over excitation enables comprehensive performance evaluation and precise parameter optimization. Practical implementation examples from the Ban Ve Hydropower Plant are presented to demonstrate the efficacy of the proposed control algorithm.

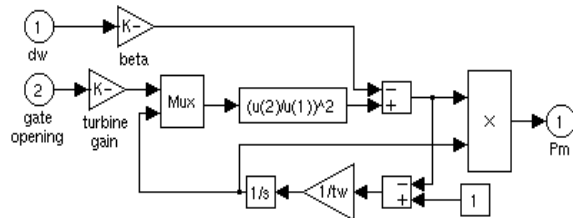
## 2. Modelling and Designing the PID Control System

The mathematical model of the turbine governor is derived based on the principles of hydraulic flow. Water passes through pipes and control valves to drive the turbine, which is mechanically coupled to the generator rotor.

As the turbine rotates, the generator produces electricity, and the output power is measured using appropriate sensors. The system compares the actual frequency with a reference value, and the frequency deviation ( $\Delta f$ ) is used as the input to the control integrator. An illustration of the control system is provided in Fig. 1.



a. Turbine governor control system



b. The hydraulic turbine non-linear model

Fig. 1. Model of turbine control system

### 2.1 Hydraulic Turbine Model

The hydro turbine is described by the water flow function and power function. In this paper, the model according to [4] is used:

$$U = K_u G \sqrt{H} \quad (1)$$

$$P = K_P H U \quad (2)$$

$$\frac{dU}{dt} = -\frac{a_g}{L} (H - H_0) \quad (3)$$

$$Q = AU \quad (4)$$

with  $U$  is water flow speed [m/s];  $G$  is ideal gate opening [%];  $H$  is working water height [m];  $H_0$  is initial water height [m];  $Q$  is water flow [ $\text{m}^3/\text{s}$ ];  $A$  is area of penstock [ $\text{m}^2$ ];  $L$  is length of penstock [m];  $a_g$  is gravitational const [ $\text{m}^2/\text{s}$ ];  $t$  is time [s].

The models described thus far are inherently nonlinear, making them unsuitable for controller design using conventional linear methods. To facilitate linear controller synthesis, a linearized model is derived by approximating the system behavior near a specific operating point. In this context,  $\Delta$  represents the deviation from the operating point, while the coefficients  $b$  are functions of the operating point and correspond to the system variables involved in the linearization process.

$$\begin{aligned} \Delta \bar{U} &= b_{11} \Delta \bar{H} + b_{12} \Delta \bar{\omega} + b_{13} \Delta \bar{G} \\ \Delta \bar{P}_m &= b_{21} \Delta \bar{H} + b_{22} \Delta \bar{\omega} + b_{23} \Delta \bar{G} \end{aligned} \quad (5)$$

The  $b_{li}$  coefficients are partial derivatives of the water flow function

$$\begin{aligned} b_{11} &= \frac{G}{2\sqrt{H}} \\ b_{12} &= 0 \\ b_{13} &= \sqrt{H} \\ b_{21} &= \frac{3}{2} \sqrt{H} \cdot G - U_{NL} A_t \\ b_{22} &= 0,5G \\ b_{23} &= A_t H^{1,5} - 0,5(\omega - 1) \end{aligned} \quad (6)$$

Supposed the  $\Delta \omega$  is relatively small in grid connecting state, the linear turbine model would be as follows:

$$\frac{\Delta \bar{P}_m}{\Delta \bar{G}} = b_{23} \frac{1 + (b_{11} - b_{13} b_{221} / b_{223}) T_w s}{1 + b_{11} T_w s} \quad (7)$$

with

$$\begin{aligned} b_{y_h} &= b_{13} b_{21} - b_{11} b_{23} \\ \Delta \bar{U} &= b_{11} \Delta \bar{H} + b_{13} \Delta \bar{G} \\ \Delta \bar{P}_m &= b_{21} \Delta \bar{H} + b_{23} \Delta \bar{G} \end{aligned}$$

### 2.2. Power-Unit Rotor Dynamics Model

Dynamics of a power unit in the turbine governing systems, in most cases, can be described by using only inertia moment of the power unit. Using Newton's second law where torques are expressed as powers

divided by the rotation speed, one can derive the following

$$G_{mayphat}(S) = \frac{\Delta\omega_N}{\Delta P - \Delta P_L} = \frac{1}{T_m s + D_p} \quad (8)$$

where  $P_L$  is mechanical power on the turbine shaft (in per unit);  $P$  is base power (in watts);  $\omega_B$  is angular velocity of the unit (in radians per second);  $D_p$  is inertia moment of the unit including all rotating parts;  $T_m$  is mechanical time constant of the unit (in seconds).

### 2.3. Speed Governing

The control structure of speed governing is show in Fig. 2.

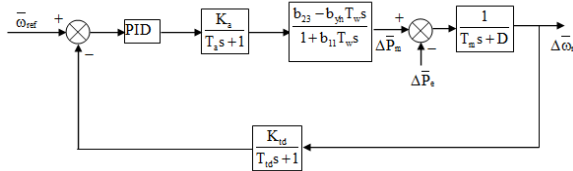


Fig. 2. Speed governing system

with the closed loop function:

$$G_\omega(s) = \frac{s + (T_a + b_{11}T_w)s^2 + T_aT_wb_{11}s^3}{b_{23}K_i + A_{\omega P_1}s + A_{\omega P_2}s^2 + A_{\omega P_3}s^3 + b_{11}T_aT_wT_m s^4} \quad (9)$$

The controller of the speed governor when designed must ensure the quality of the system according to the National Technical Regulation on Electrical Engineering QCVN-2015/BCT and other technical requirements:

- Static deviation of frequency in normal operating mode is not more than  $\pm 1\%$ ;
- Maximum speed of the speed governor is not more than 50% of the rated speed;
- Delay time of the controller's action is not more than 0.2s;

The parameters of the controller are determined based on the desired polynomial, the rule for selecting parameter values for this polynomial:  $(s^2 + 2\xi\beta_n s + \beta_n^2)$  and the optimal coefficients of the desired polynomial are constructed according to the ITAE (*Integral of Time multiplying the Absolute value of the Error*) criterion by the experiment of Dorf & Bishop [2] with

Table 1. Desired polynomials

Order	Desired polynomials $d_k(s)$
1	$d_1(s) = [s + \beta_n]$
2	$d_2(s) = [s^2 + 1,4\beta_n s + \beta_n^2]$
3	$d_3(s) = [s^3 + 1,75\beta_n s^2 + 2,15\beta_n^2 s + \beta_n^3]$

The  $K_p$ ,  $K_i$ ,  $K_d$  of PID controller and  $c_3$  are a function of  $c_0$ ,  $c_1$ ,  $c_2$ . In which:

$$K_p = \frac{b_{22}b_{23} + b_{yh}T_aT_mT_w^2c_0 + b_{23}(b_{11}T_aT_mT_wc_1 - D)}{b_{23}^2} \quad (11a)$$

$$K_I = \frac{b_{11}T_aT_mT_wc_0}{b_{23}} \quad (11b)$$

$$c_3 = f(c_0, c_1, c_2) \quad (11c)$$

$$p_{kd\omega_1} = D - b_{11}T_aT_mT_wc_1 + 2b_{11}^2T_aT_mT_w^2c_0 \quad (11d)$$

$$p_{kd\omega_2} = DT_a + T_m + b_{12}b_{21}T_w - b_{11}T_aT_mT_wc_2 + b_{11}^2T_aT_mT_w^2c_1 - b_{11}^3T_aT_mT_w^3c_0 \quad (11e)$$

### 2.4. Simulation of the designed PID controller

The turbine system's parameters is shown in Table 2

Table 2. Turbine parameters

Names	Symbol	Values
Generator rated power	$Pfdm$	160 MW
Stator rated voltage	$U1dm$	15.75 KV
Rated frequency	$fdm$	50 Hz
Rated speed	$nf dm$	150 v/p
Calculated water head	$Htt$	66,5 m
Maximum water flow through turbine	$Qmax$	188 m <sup>3</sup> /s
Allowable speed	$nTlt$	(225) v/p
Penstock length	$Lp$	179 m
Pentstock cross-sectional area	$Ap$	3,6 m <sup>2</sup>

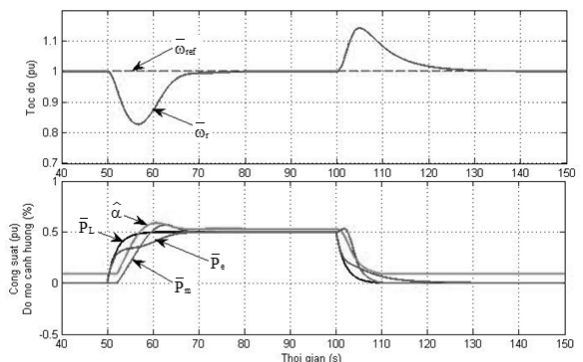


Fig. 3. Response of the speed loop with exact parameters

The simulation results of the speed loop with the designed controller shown in equation [11] is presented in Fig. 3, in which:

- Transition time 15s, Deceleration when loading is 17%.
- Overspeed when rejecting 100% load is 15%.
- Steady state error is 0.
- Response is non-oscillating.

The simulation is tested when the load is being suddenly changed at the time of 300s, and the water head is 20% differences, the response is in Fig. 4.

These results lead to the conclusion that when system inputs and outputs remain stable, the PID controller is capable of meeting control quality requirements. However, in scenarios where the water head and electrical load vary significantly (up to 20%), the fixed-parameter PID controller fails to maintain a new equilibrium. Under such conditions, the system experiences pronounced fluctuations around the desired setpoint, indicating a loss of control effectiveness.

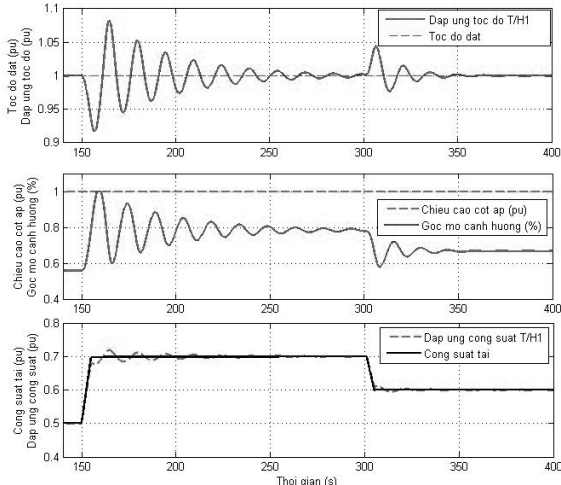


Fig. 4. Speed response at load changed with 20% head difference

### 3. Neural Network PID Controller

The Adaptive Neural Network PID Controller (PID-NN) integrates the classical Proportional Integral Derivative (PID) control strategy with a neural network framework, leveraging the Brandt-Lin Algorithm to adaptively tune the controller parameters. This approach is particularly effective for controlling nonlinear or time-varying systems, such as turbine power systems, where traditional PID controllers may struggle due to fixed gains and complex dynamics.

#### 3.1. Brandt-Lin Algorithm Neural Network

The Brandt-Lin algorithm provides a framework for adapting the connection weights of a neural network to optimize system performance. For a system with dynamics described by mathematical equations,

the algorithm adjusts the weights to minimize a performance index, ensuring stable and predictable system behavior.

**Key Concept:** The performance index  $E$ , which depends on system outputs ( $y_1, \dots, y_n$ ) and control inputs ( $u_1, \dots, u_n$ ), decreases over time when the weights are updated according to the adaptation rule. This rule ensures that the system converges to a stable state, provided the system's Jacobian determinant is non-zero in the region of interest.

If the system dynamics and performance index involve instantaneous functions, the adaptation rule simplifies to a multiplication operation, making the computation more straightforward. The simplified equations for weight adaptation are as follows:

- **Weight Update Rule:** The connection weights are adjusted based on the adaptation coefficient and system dynamics.
- **Mathematical Representation:**

$$w = w - \eta \cdot \frac{\partial E}{\partial w}$$

where  $\eta$  is the adaptation coefficient, and  $\frac{\partial E}{\partial w}$  represents the gradient of the performance index with respect to the weights. This approach is versatile and can be applied to various systems, including neural networks, as illustrated in the Fig. 5 diagram.

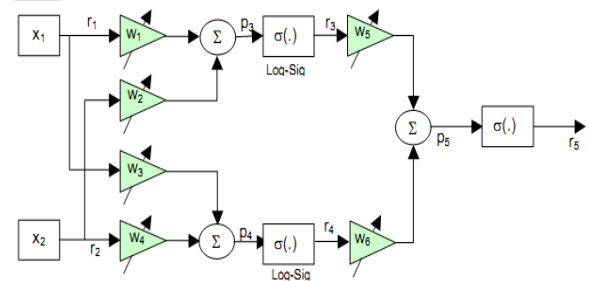


Fig. 5. A simple neural network

The weight adaptation becomes as shown in [7]:

$$w_s = r_{pre_s} (\phi_{post_s} \sigma(-p_{post_s}) + \gamma f_{post_s}) \quad (12)$$

#### 3.2. Adaptive Neural Network Controller PID-NN

The configuration of the neural network controller is further described in Fig. 6.

**Input Layer:** Three neurons corresponding to the P, I, and D components of the error. Each neuron processes its input using an activation function

**Output Layer:** One neuron that produces the control signal  $u(t)$  using a linear activation function for direct control action.

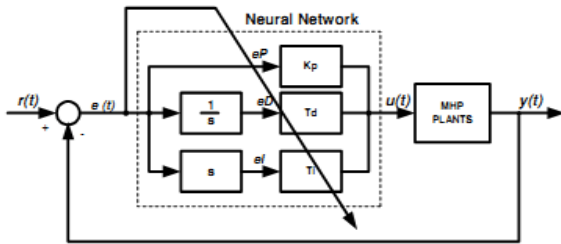


Fig. 6. Neural network controller

- Weights

In a simplified structure, the network may directly connect the three input neurons to the output neuron via weights  $w_1, w_2, w_3$ , representing the proportional, integral, and derivative gains, respectively.

- Mathematical Representation

Let the inputs to the neural network be:

$$x_1 = e(t), \quad x_2 = \int e(t) dt, \quad x_3 = \frac{de(t)}{dt} \quad (13)$$

The input to the output neuron (membrane potential) is:

$$p_{\text{out}} = w_1 x_1 + w_2 x_2 + w_3 x_3 \quad (14)$$

The output (control signal) is:

$$u(t) = p_{\text{out}} \quad (\text{linear activation})$$

or, if a hidden layer is used:

$$p_{\text{hidden},i} = \sum_{j=1}^3 w_{ij} x_j, \quad r_{\text{hidden},i} = \sigma(p_{\text{hidden},i}), \quad u(t) = \sum_i w_{\text{out},i} r_{\text{hidden},i} \quad (15)$$

The error is defined as:

$$E = \frac{1}{2} (r(t) - y(t))^2 = \frac{1}{2} e(t)^2 \quad (16)$$

- Brandt-Lin Algorithm in PID-NN

The Brandt-Lin Algorithm is used to train the neural network by adapting its weights to minimize the error  $E$ , the algorithm uses local computations at each neuron, making it suitable for real-time control in a turbine power systems.

Adaptation Law, the weight update rule is:

$$\dot{w}_s = -\alpha_s \frac{dE}{dw_s} \quad (17)$$

where:

$w_s$ : Weight of synapse  $s$ ;

$\alpha_s$ : Adaptation coefficient (learning rate) for synapse  $s$ ;

$\frac{dE}{dw_s}$ : Total derivative of the error with respect to the weight;

For the PID-NN, the weights correspond to the PID gains ( $w_1, w_2, w_3$  for P, I, D terms). The error gradient is computed as:

$$\frac{dE}{dw_s} = \frac{\partial E}{\partial p_{\text{out}}} \cdot \frac{\partial p_{\text{out}}}{\partial w_s} \quad (18)$$

where:

- $\frac{\partial E}{\partial p_{\text{out}}} = -(r(t) - y(t)) \cdot \frac{\partial y}{\partial u}$ , accounting for the plant's response.
- $\frac{\partial p_{\text{out}}}{\partial w_s} = x_s$ , the input associated with the weight (e.g.,  $e(t), \int e(t) dt, \frac{de(t)}{dt}$ ).

In the Brandt-Lin framework, the adaptation simplifies to:  $\dot{w}_s = \alpha_s x_s (\lambda_{\text{out}} \phi_{\text{out}} \sigma'(p_{\text{out}}) + f_{\text{out}})$

where:

- $x_s$ : Presynaptic input (P, I, or D term);
- $f_{\text{out}} = r(t) - y(t)$ : Feedback signal (error);
- $\phi_{\text{out}} = \sum_s \alpha_s w_s \dot{w}_s$ : Implicit feedback from outgoing synapses;
- $\sigma'(p_{\text{out}})$ : Derivative of the activation function (for linear output,  $\sigma' = 1$ );

For a linear output neuron the adaptation simplifies further:  $\dot{w}_s = \alpha_s x_s (r(t) - y(t))$ .

This resembles gradient descent, adjusting weights proportionally to the error and input.

- Application to PID-NN

**Weights as PID Gains:** The weights  $w_1, w_2, w_3$  directly represent the proportional, integral, and derivative gains. The Brandt-Lin Algorithm tunes these weights online to optimize control performance.

**Adaptation Rate ( $g$ ):** The learning rate  $g$  (denoted as  $\alpha_s$  in the algorithm) controls how quickly the weights adapt. A smaller  $g$  ensures stability but slows adaptation, while a larger  $g$  speeds up adaptation but risks instability.

**Training Process:** The neural network learns by continuously updating weights based on the error  $e(t)$ , allowing the controller to adapt to changes in the plant (e.g., turbine dynamics) or disturbances (e.g., load changes).

### 3.3. Simulation of the NN-PID controller

The simulation is implemented in the following cases:

- **Case 1 (T/H1):** The water head is stable, the electric load changes suddenly. Assuming that the system is operating stably, then at  $t = 150$  s the load capacity suddenly increases from 0.5 (pu) to 0.7 (pu), then at  $t=300$ s the load capacity decreases again to 0.6 (pu);

- *Case 2 (T/H2)*: The water head increases and the electric load changes. Assuming that the system is stable at the equilibrium point, then at  $t = 250$  s, the water head of the system increases rapidly from 66.5 m to 70 m

The comparison of between the quality of PID and NNC is described in Table 3

Comparison of speed loop response when using PID controller and NNC controller as show Fig. 7 for T/H1 and Fig. 8 for T/H2

Table 3. Quality parameters of PID and NNC controllers in speed loop

Case	Controller	$t_p$ (s)	$\delta_{max}$ (%)	n	ss
Case 1	PID	-	5	-	-
	NNC	30	4,6	1	0,02
Case 2	PID	-	6	-	-
	NNC	30	5	1	0,02

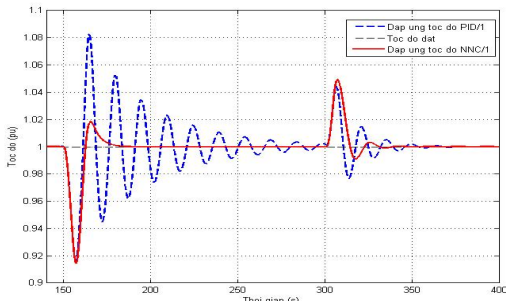


Fig. 7. Speed response in T/H1

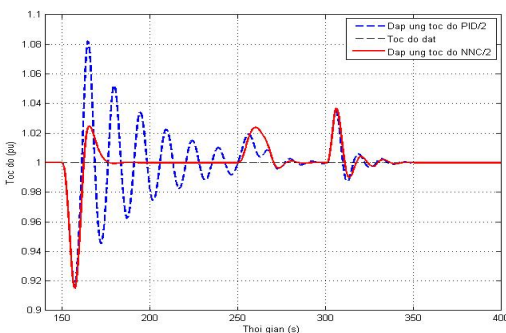


Fig. 8. Speed response in T/H2

The simulation results clearly indicate that when the electrical load increases by 5% of the nominal value, the frequency deviation reduces after a brief transient period. With a conventional PID controller,

the system takes approximately 50 seconds to settle and exhibits noticeable oscillations. In contrast, the PID-NN controller achieves a faster response with a transition time of 30 seconds and eliminates oscillations entirely.

#### 4. Experimental Results

Experimental verification of the digital governor control system is made on the 160MW turbine of BanVe hydro-power plant in Vietnam. Digital control system with PLC S7 1500 as shown in Fig. 9 is applied to meet the strict industrial requirement. The hardware, which integrates the main controller and the Human Machine Interface (HMI), is applied to develop a dynamic real-time system. The hardware consists of a redundant S7 1512 controller, a 12-inch HMI, interface, a Profibus interface, a 24 V DC power supply, 32 digital input/output channels, 4 channels analog input (16 bits resolution, 4-20mA) is used.



Fig. 9. The S7 1500 PLC turbine control system

The experiment data has been shown on the Fig. 10 to Fig. 13. The results have proved the effectiveness of proposed controllers. Due to the length limit of the paper, only the most convincing figures are presented.

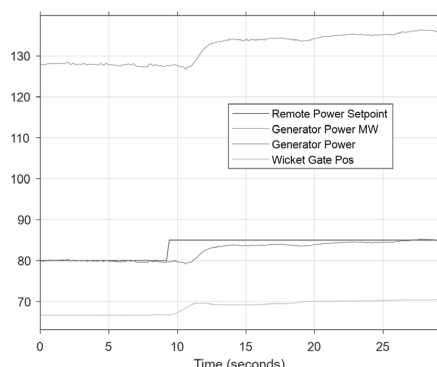


Fig. 10. Speed increases from 80% to 85%

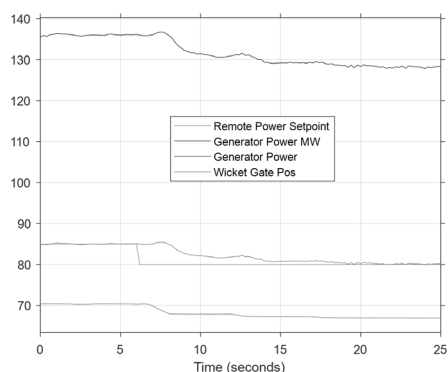


Fig. 11. Speed decreases from 85% to 80%

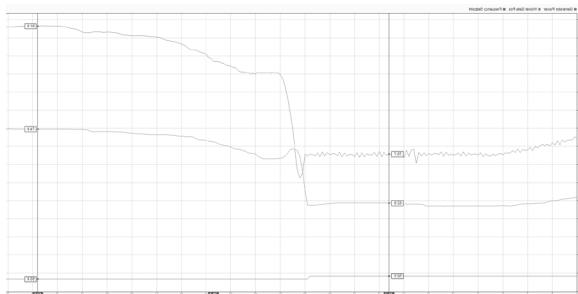


Fig. 12. Frequency changes suddenly from 50.5Hz to 50Hz

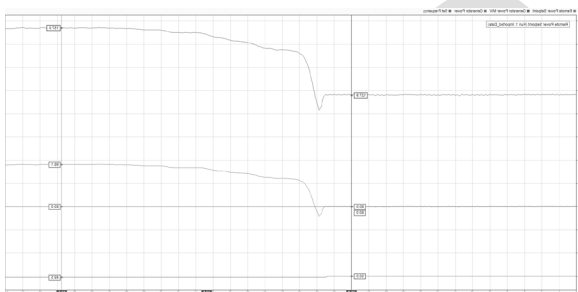


Fig. 13. Frequency changes suddenly from 50Hz to 49.5Hz

The experiments were conducted in accordance with Circular 31/2019/TT-BCT, using a 5% speed setpoint and a sudden 0.5 Hz frequency change to evaluate the rapid response of the turbine controller. As observed, all requirements were satisfied, with the error approaching zero in every test case.

## 5. Conclusion

The effectiveness of the proposed governor control system was verified through simulation tools, and the accuracy of the plant simulation model was confirmed via experimental validation. This study demonstrates that, with accurate turbine parameters, conventional PID control can meet system performance requirements. One of the key advantages of PID controllers is their simplicity in implementation and commissioning.

Furthermore, an adaptive neural network approach using the Brandt-Lin algorithm was applied to train the neural network structure in the NN-PID controller for turbine-generator speed control, as illustrated in Fig. 5. With an adaptation rate of  $\gamma = 100$ , simulation results after approximately 30 seconds indicate significant improvements in the network's link weights ( $W$ ) and error ( $E$ ), highlighting the effectiveness of the training process.

Simulation results show that the NN-PID controller delivers a superior response to power system load changes, achieving a 30 second transition time with no oscillations. In comparison, the traditional PID controller exhibits a longer 50 second transition time and noticeable oscillations.

Despite these advantages, most hydropower plants currently continue to rely on conventional PID controllers. The NN-PID controller is proposed as a more effective tool for designing and implementing high-quality speed control systems for hydraulic turbines.

## Acknowledgments

The EVN and Genco1 provided financial support to carry out this research.

## References

- [1] P.Kundur, Power System Stability and Control, NewYork, Tata McGraw-Hill, 1994.
- [2] Richard C. Dorf, Robert H. Bishop Modern Control Systems, Prentice Hall, 2008
- [3] J.A. Jaleel, T.P. Imthias Ahammed, Simulation of artificial neural network controller for automatic generation control of hydro electric power system, IEEE Region 10th Conference Publication, Tencon 2008, pages 1-4.  
<https://doi.org/10.1109/TENCON.2008.4766636>
- [4] K. S. Narendra and K. Parthasarathy, Identification and control of dynamical systemsusing neural networks, IEEE Transactions on Neural Networks, Vol. 1, pp 1-27, 1990.  
<https://doi.org/10.1109/72.80202>
- [5] F. C. Chen and H. K. Khalil, Adaptive control of nonlinear systems using neural networks, IEEE proceedings on the 29th Conference on Decision and Control, Vol.44, TA-12-1-8:40, 1990.
- [6] T. Yamada and T. Yabuta, Neural network controller using autotuning method for nonlinear functions, IEEE Transactions on Neural Networks, Vol. 3, pp 595-601, 1992.  
<https://doi.org/10.1109/72.143373>
- [7] M.Hanmandlu, Himani Goyal, Proposing a new advanced control technique for micro hydro power plants, Journal of Electrical Power and Energy System, 30(2008), pages 272-282.  
<https://doi.org/10.1016/j.ijepes.2007.07.010>

[8] R. D. Brandt, F. Lin, Adaptive interaction and its application to neural networks, Elsevier, Information Science 121, pp 201-215 1999.  
[https://doi.org/10.1016/S0020-0255\(99\)00090-0](https://doi.org/10.1016/S0020-0255(99)00090-0)

[9] O. Quiroga, J. Riera and C. Batlle, Identification of partially known models of the Susqueda hidroelectric power plant, Latin American Applied Research, 2003, Vol. 33 (No. 4), pp. 387-392.

In Press